Supporting information for: Statics and Dynamics of Free and Hydrogen-Bonded OH Groups at the Air/Water Interface

Ana Vila Verde,[*,†,¶] Peter G. Bolhuis,[*,†] and R. Kramer Campen[*,‡]

Van't Hoff Institute for Molecular Science, University of Amsterdam, Amsterdam, PO Box 94157 1090 GD Amsterdam, The Netherlands, and Fritz Haber Institute of the Max Planck Society, Faradayweg 4–6, 14195 Berlin, Germany

E-mail: ana.vilaverde@mpikg.mpg.de; p.g.bolhuis@uva.nl; r.k.campen@fhi-berlin.mpg.de

[*]To whom correspondence should be addressed

[†]University of Amsterdam

[‡]Fritz Haber Institute of the Max Planck Society

[¶]Currently at the Max Planck Institute of Colloids and Interfaces, Theory and Bio-Systems Department, Wissenschaftspark Potsdam-Golm, Am Mühlenberg 1 OT Golm 14476 Potsdam, Germany; also at the University of Minho, Physics Center, Campus de Gualtar, 4710-057 Braga, Portugal.

Simulation files

The necessary CHARMM-compatible parameter and topology files to run simulations using the TIP4P/2005 water model[1–3] with NAMD are not available in standard distributions, so they are given in the supporting information as separate files: par_TIP4P2005.txt and top_TIP4P2005.txt.

Fraction of interfacial water molecules with two free OH groups is very small

The fraction of water molecules with one ($f_{sf}(z)$) or two ($f_{df}(z)$) free OH groups at each position in the water slab is calculated as

$$f_{sf}(z) = \frac{\langle n_{sfH2O}(z) \rangle}{\langle n_{tH2O}(z) \rangle} \tag{1}$$

and

$$f_{df}(z) = \frac{\langle n_{dfH2O}(z) \rangle}{\langle n_{tH2O}(z) \rangle} \tag{2}$$

Here $n_{sfH2O}(z)$ is the number of water molecules at each position z with a single free OH group, $n_{dfH2O}(z)$ the number of molecules with two free OH groups and $n_{tH2O}(z)$ the total number of water molecules at that position. These two quantities are shown in Figure 1 for the SPC/E and the TIP4P/2005 water models and the HB2 hydrogen bond criteria. Figure 1(a) indicates that the fraction of water molecules with two free OH groups is almost zero in the bulk, becoming high (> 0.2) only in the outermost regions of the interface. As these regions have very low density, the total population of interfacial water molecules with two free OH groups is only 4%. Figure 1(b) further confirms that most of the free OH groups at the interface belong to water molecules where the second OH group is hydrogen bonded.

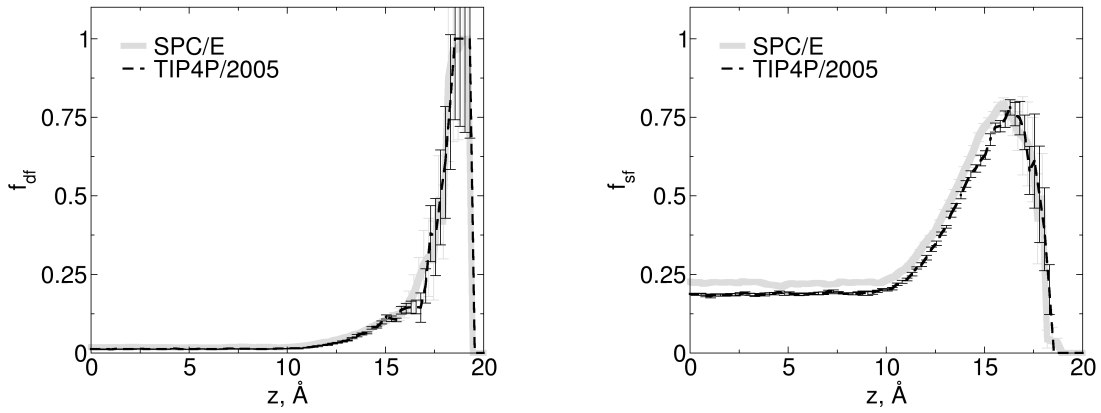

(a) (b)

Figure 1: Fraction of water molecules with (a) two and (b) one free OH groups at each position z of the water slab for the two water models and the HB2 criteria. The error bars indicate the statistical uncertainty calculated as described in the body of the paper.

Residence time of waters at the interface is ≈ 10 ps

To estimate the residence time, we first compute the probability $P_I(\tau)$ that a water molecule remains continuously at the interface during at least time τ

$$P_I(\tau) = \langle n_I(0) n_I(\tau) \rangle \tag{3}$$

where $n_I(\tau) = 1$ if a water molecule belongs to the interface during the interval $[0, \tau]$ and is zero if the molecule left the interface at any time during that interval and the average is over all $n_I(0) = 1$.

The resulting decay curves for the SPC/E and TIP4P/2005 water models are well described by a bi-exponential function. We thus fitted the curves with a bi-exponential $b_0 \exp(-x/b_1) + b_2 \exp(-x/b_3)$ to extract the residence times b_1 and b_3. The decay curve is dominated ($b_0 = 0.8$) by the long-time decay, characterized by the residence times $b_1 = 12$ ps (SPC/E) and $b_1 = 15$ ps (TIP4P/2005). The less important ($b_2 = 0.2$) fast decay is characterized by a decay constant of $b_3 = 1$ ps for both water models. The overal residence time is calculated[4–7] as $\tau = (b_0 * b_1 + b_2 * b_3)/(b_0 + b_2)$ and is 10 ps (SPC/E) or 13 ps (TIP4P/2005). We note that our long-time decay

constants are of the same order as those obtained from ab initio molecular dynamics simulations[8] (7.5 ps) but much larger than the value reported from simulations using the SPC/E water model[6] (2 ps). The origin of the discrepancy between our residence times and those found by Taylor et al.[6] is presumably related to their more spatially restrictive definition of the interface and shorter cut offs for calculation of non bonded interactions.

Orientation of interfacial free OH groups is sensitive to HB definition

The distribution of angles θ of free and bonded SPC/E OH groups at the interface relative to the surface normal is shown in Figure 2 for three different hydrogen bond criteria. It is apparent that the orientation of the bonded OH groups is insensitive to changes in hydrogen bond criteria, while the orientation of the free OH groups is quite sensitive to this choice. These results indicate that the most stable free OH groups (i.e. those that do not form even weak hydrogen bonds (HB3 criteria)) are oriented closer to the surface normal than the less stable free, interfacial, OH groups.

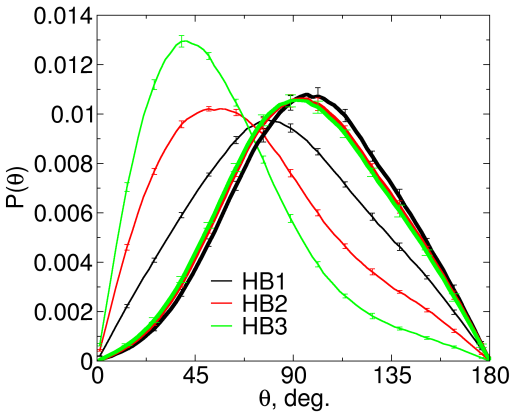

Figure 2: Probability distribution function $P(\theta)$ of interfacial SPC/E OH groups either free (thin lines) or hydrogen bonded (thick lines), for three hydrogen bond criteria.

The orientation of OH groups at the air/water interface is similar, but not identical, to that near an extended hydrophobic surface

The air-water interface is often assumed to be similar to extended interfaces between water and hydrophobic surfaces. It is thus important to compare the orientation of OH groups at the air-water interface with their orientation at the hydrophobic-water interface; such an interface was recently investigated by Stirnemann et al.[9] using very similar models to those used here. To facilitate this comparison, in Figure 3 we present the normalized orientation distribution at the air-water interface in a format that allows direct comparison with Fig. 1 in Stirnemann et al.[9] Inspection of this figure

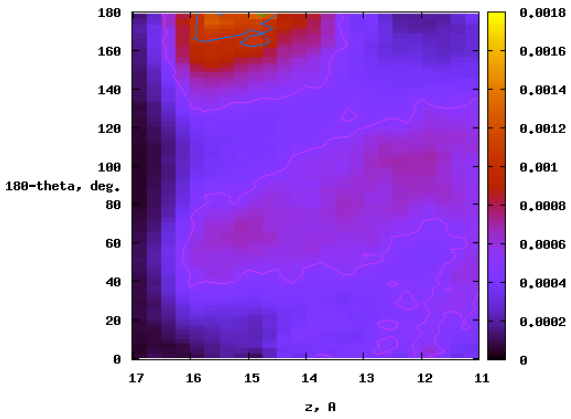

Figure 3: Normalized orientation distribution $P(\theta,z)/\sin(\theta)$. Note that the x axis is inverted so that air is on the left- and bulk water on the right-hand-side, and that the y axis is given as $180-\theta$ so that direct comparisons with Fig. 1 of Stirnemann et al.[9] are possible.

confirms that the free OH groups at the air-water interface point out ($180-\theta \approx 180$) and that the bonded OH groups in the outer layers of the interface are roughly tangent to that interface ($50^\circ < 180-\theta < 120^\circ$), similarly to what was observed for the hydrophobic-water interface.[9] In contrast to what was found for the hydrophobic-water interface, however, we do not observe a population of bonded OH groups with a peak at $180-\theta \approx 0$.

Free Energy Landscape of the hydrogen-bonded state at the Interface vs. in Bulk

Hydrogen bonds have similar strength at the interface and in the bulk

As described in the main text, we compute the 2-dimensional probability density $P_{HB}(d,\varphi)$ of the O$\cdots$O distance (d) and O-H$\cdots$O angle (φ) separately for central O-H groups located at the interface or in the bulk, using a cut off distance and angle the HB3 criteria. These probability densities are shown in Figure 4 for the SPC/E water model; the TIP4P/2005 water model yields very similar results (not shown). Clearly, differences between these two plots are not apparent by inspection; hence we fitted a bivariate Gaussian distribution to each of them to obtain estimates of the mean and standard deviation of d and φ. The fitted function has the form

$$P_{HB}(d,\varphi) = \kappa \exp\left(-\frac{1}{2(1-\rho^2)}\left[\left(\frac{d-\mu_d}{\sigma_d}\right)^2 - \left(\frac{2\rho(d-\mu_d)(\varphi-\mu_\varphi)}{\sigma_d\sigma_\varphi}\right) + \left(\frac{\varphi-\mu_\varphi}{\sigma_\varphi}\right)^2\right]\right) \quad (4)$$

where μ is the mean and σ is the standard deviation for d and φ, ρ is the covariance of d and φ and κ is a normalization constant. The results of the fit are discussed in the main text.

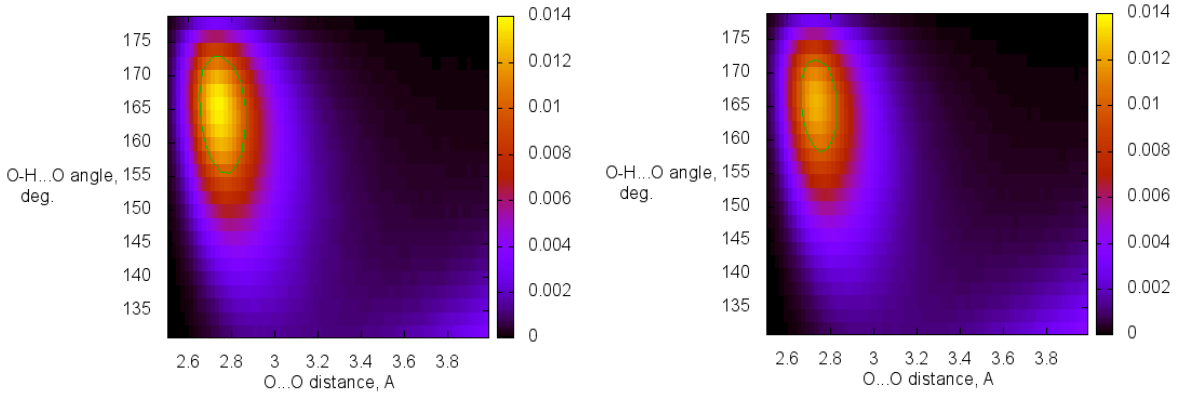

(a) (b)

Figure 4: Two-dimensional probability density $P_{HB}(d,\varphi)$ for water molecules (a) at the interface or (b) in the bulk, for the SPC/E water model.

Increase of O$\cdots$O distance for hydrogen-bonded waters at the interface qualitatively agrees with experiment and reported simulations

Saykally and coworkers found, in a 2002 EXAFS study of a liquid water microjet, that the O$\cdots$O distance at the air/water interface is 6% larger than in bulk.[10] Subsequent computational studies of the air/water interface, including classical (both fixed charge and polarizable), and AIMD approaches have found that, in general, classical approaches lead to an O$\cdots$O distance in interfacial water that is smaller than in bulk by $\approx 1\%$ while AIMD (employing the BLYP functional) leads to a similar magnitude interfacial expansion.[7,8] This observation has been interpreted as indicating that classical models are likely not able to capture accurately the electronic structure of interfacial water. Our study, in which both SPC/E and TIP4P/2005 water models produce a slight *increase* in O$\cdots$O distance in interfacial water relative to the bulk ($< 0.5\%$) and existing reports of a similar trend also for SPC/E water[11] indicate that the SPC/E and the TIP4P/2005 model *do* qualitatively agree with experimental estimates of air/water interface surface relaxation. Clearly, however, while qualitatively in agreement with experiment our $< 0.5\%$ expansion in O$\cdots$O distance quantitatively differs from 6%. More recent work by Saykally and coworkers has emphasized the challenges in correctly interpreting micro jet experiments and has emphasized that their 2002 surface expansion estimate should be revisited.[12] To our knowledge more recent EXAFS studies have not been published thus we do not here address this discrepancy further.

Lifetimes of the hydrogen bonded and the free states

The lifetime of the free and the hydrogen bonded states at the interface or in the bulk was estimated by calculating the function $C_y(\tau)$:

$$C_y(\tau) = \left\langle n_y(0) n_y(\tau) \right\rangle \tag{5}$$

where $n_y(\tau) = 1$ if an OH group is free ($y = free$) or bonded ($y = bond$) at time τ, and the average is over all $n_y(0) = 1$. The resulting curves for the decay of the free and hydrogen-bonded states are shown in Figure 5 for the HB2 criteria. These curves are poorly described by single exponentials, but double exponentials of the form $a * \exp(-\tau/\tau_a) + b\exp(-\tau/\tau_b) + c$ are sufficient to adequately describe them. The constant c is set to zero when fitting the $C_{bond}(\tau)$ functions because the probability of any given hydrogen-bond surviving for infinite times is zero. In contrast, the end-level of the function $C_{free}(\tau)$ is the average fraction of free OH groups at the interface, so c is a fitting parameter in this case. For both the interface and the bulk, we find that the τ_a and τ_b terms have comparable amplitudes but the shorter decay time of the two is always of order 0.01 ps. As such a short time scale is associated with librational motion of OH groups that only very transiently interrupts the bonded or free states, the lifetime of the free and bonded states reported in the main text is simply the largest of the two decay times obtained from the fit.

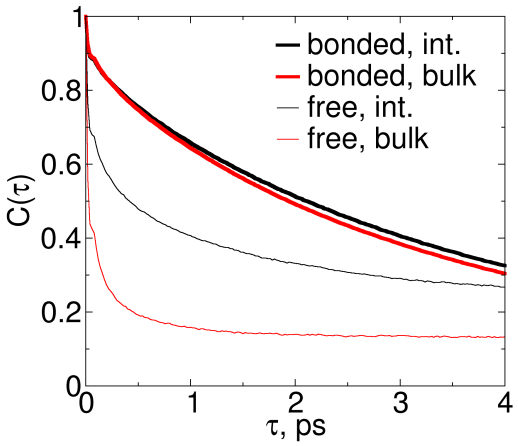

Figure 5: Decay of the SPC/E free or hydrogen bonded states (HB2 criteria) of OH groups that at $t = 0$ belong to the bulk or the interface, as measured by the autocorrelation function $C(\tau)$.

Longer-lived, free OH groups at the interface have smaller average values of θ and narrower orientational distributions

In the main text of the paper we show that the lifetime of free OH groups at the interface depends on their orientation in θ. We illustrate this dependence in two complementary ways: we calculate the orientation distribution for interfacial OH groups that remain free for different times (see Figure 6(a)) and the decay curves for the free OH state – as quantified by $C_f(\tau)$ – for interfacial OH groups that at t=0 have different θ orientation (see Figure 6(b)). These figures illustrate that the lifetime of free OH groups at the interface is larger for more upright subpopulations i.e., longer-lived free OH groups at the interface have narrower distributions in θ and, on average, form smaller angles with the surface normal.

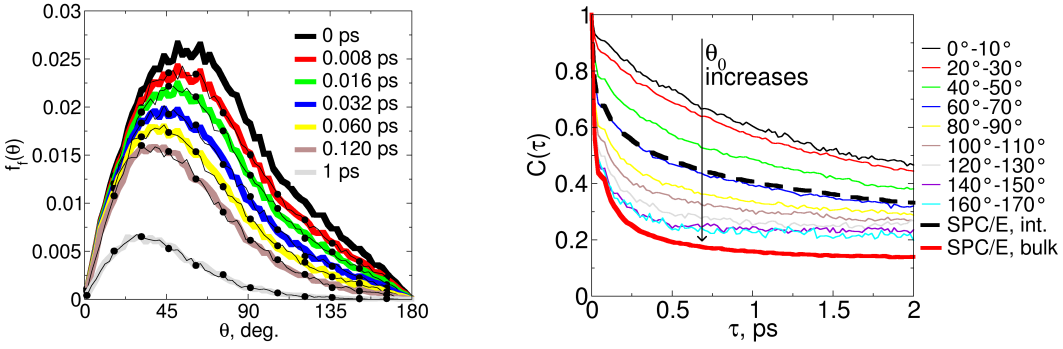

(a) (b)

Figure 6: (a) Magnitude and orientation of subpopulations of interfacial SPC/E OH groups that remain free for the indicated times, expressed as the fraction $f_f(\theta)$ of the total population of OH groups that is free at $t = 0$. The thick black curve is the distribution for the total population of free OH groups at $t = 0$. The remaining thick curves indicate the $f_f(\theta)$ at $t = t$ for the subpopulation of OH groups that remain continuously free between 0 and t; the thin black curves quasi-overlapping with each thick curve indicate the $f_f(\theta)$ for the same subpopulation of OH groups, but at $t = 0$. (b) Decay of the free state of interfacial SPC/E OH groups, as measured by the $C_f(\tau)$ function presented above, as a function of their orientation in θ at t=0. For comparison, the decay curves for free OH groups in the bulk (thick red curve) and the average decay of the entire population of interfacial, free, OH groups (thick black curve) already presented in Figure 5 are also shown.

Hydrogen bond exchange mechanism

The mechanism proposed by Laage and Hynes for hydrogen bond exchange in the bulk is illustrated in Figure 7.[13] For a description of the mechanism see the main text.

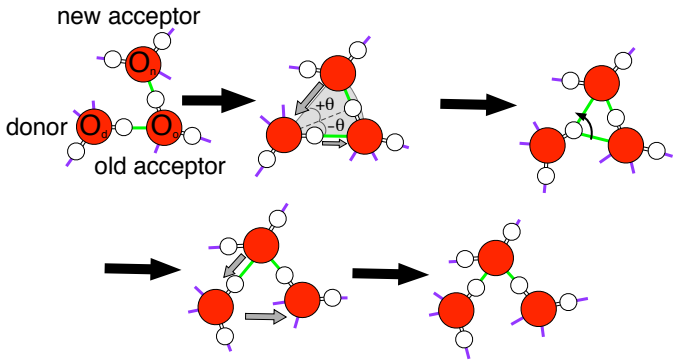

Figure 7: Angular jump mechanism of hydrogen bond exchange after Laage and Hynes.[13] The necessary reaction coordinates for the mechanism are the distance both between the hydrogen bond donor and old hydrogen bond acceptor ($O_d \cdots O_o$) and donor and the new hydrogen bond acceptor ($O_d \cdots O_n$) as well as the jump angle (ϑ). ϑ is defined to be zero at the bisector of the $\angle O_o - O_d - O_n$ angle. Image originally published by Vila Verde and Campen.[14]

Hydrogen bond exchange mechanism at the interface is indistinguishable from the bulk

As mentioned in the main text, the hydrogen bond exchange mechanism is characterized by changes in the $O_d \cdots O_o$ and $O_d \cdots O_n$ distances, and in the angle ϑ. Here we show the average trajectories in these coordinates (Figure 8) and also the distribution of these trajectories (Figure 9). Inspection of Figures 8 and 9 confirms that oxygen-oxygen distances and the angle ϑ evolve similarly for hydrogen bond exchanges at the interface or in the bulk.

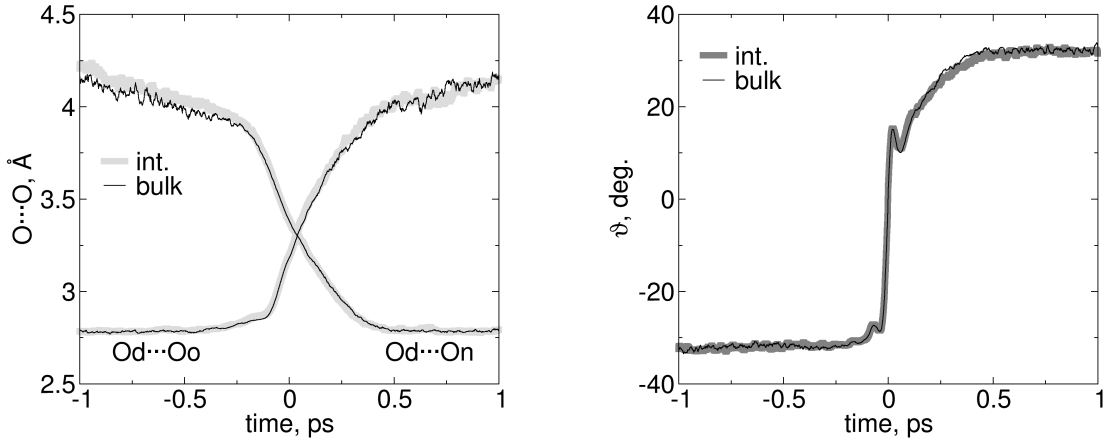

(a) (b)

Figure 8: Average change in (a) oxygen-oxygen distances and (b) ϑ during hydrogen exchange (HB1 criteria) for SPC/E water at the interface and in the bulk. The average jump size associated with hydrogen-bond exchange is $\Delta\vartheta = 64 \pm 1^\circ$ for both water subpopulations, and the average jump duration is ≈ 0.2 ps.

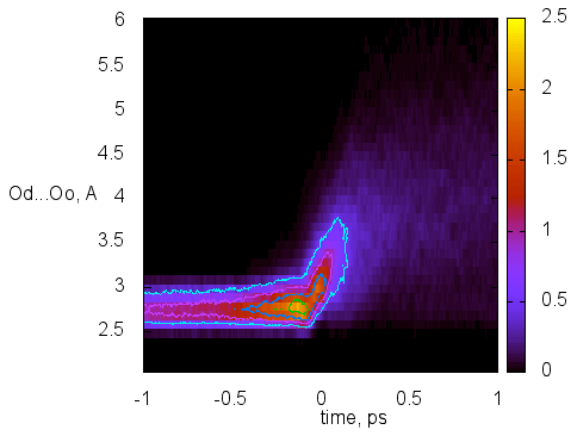

(a) $O_d \cdots O_o$ distribution, bulk.

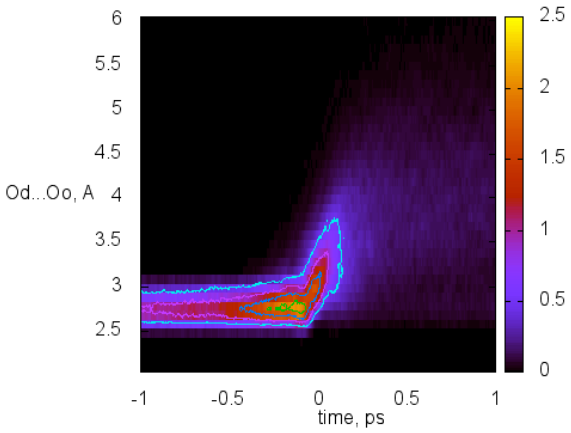

(b) $O_d \cdots O_o$ distribution, interface.

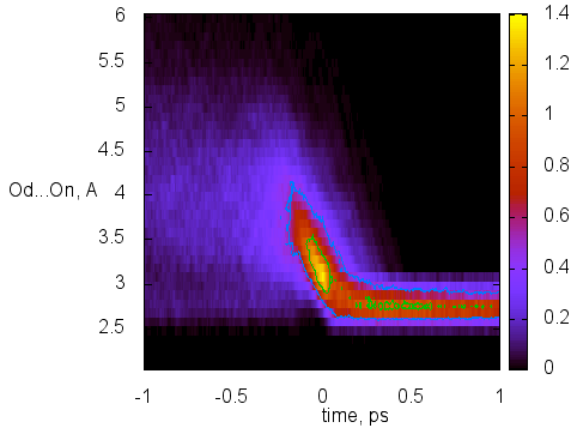

(c) $O_d \cdots O_n$ distribution, bulk.

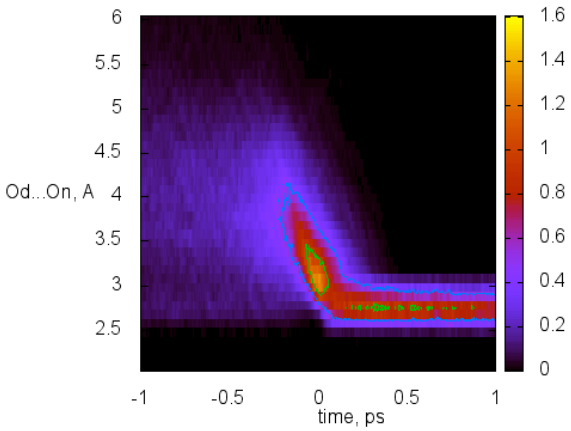

(d) $O_d \cdots O_n$ distribution, interface.

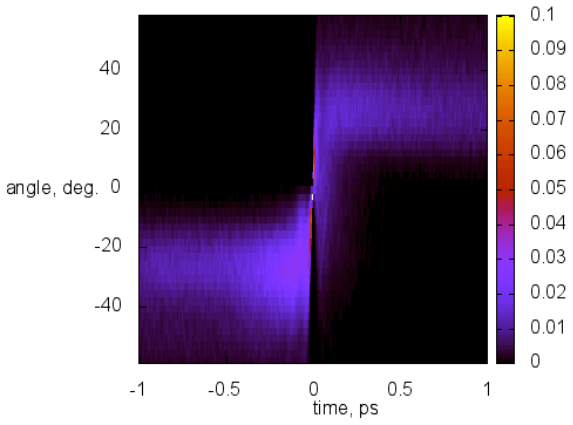

(e) ϑ distribution, bulk.

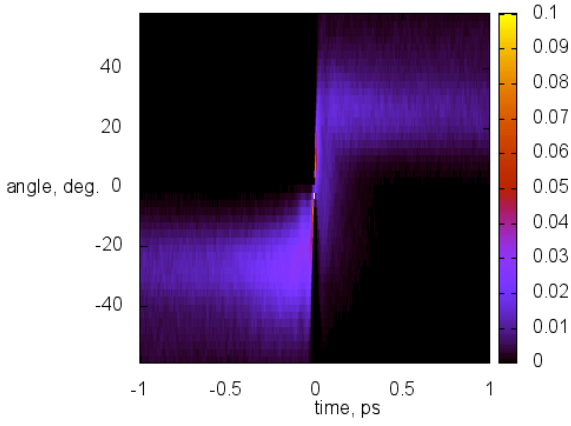

(f) ϑ distribution, interface.

Figure 9: Distribution of oxygen-oxygen distances and the ϑ angle during hydrogen exchange for SPC/E water at the interface and in the bulk. The lack of time symmetry in the ϑ distributions arises because $t = 0$ is defined as the first instant that ϑ is larger than 0; because of fluctuations, there is a small probability that ϑ may transiently become negative before a stable product state is established.

Frame decay is faster at the interface than in the bulk

The reorientation of the O-H$\cdots$O axis that occurs between hydrogen bond exchanges is shown is shown in Figure 10. These results are discussed in the main text of the paper.

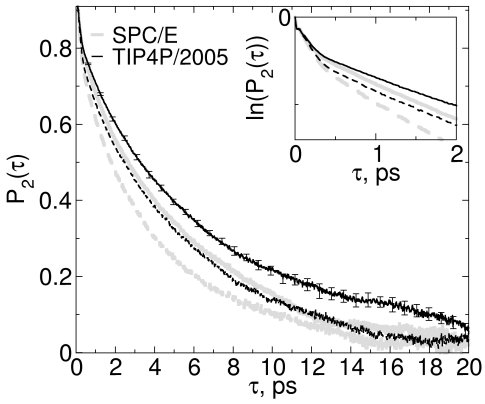

Figure 10: Frame reorientation $P_2(\tau)$ between hydrogen bond exchanges at the interface (dashed lines) or in the bulk (continuous lines) for SPC/E or TIP4P/2005 water. The inset shows $\ln(P_2(\tau))$ for short time scales.

Mean squared displacement plots: translation is faster at the interface

We calculate the 3D mean squared displacement for SPC/E water molecules that at $t = 0$ are either at the interface or in the bulk, without imposing any conditions on their position at $t > 0$. Our results, shown in Figure 11, indicate that translation is faster at the interface than in the bulk in all regimes (ballistic, for $t < 200$ fs; subdiffusive, for $0.2 < t < 5$ ps; and diffusive, $t > 5$ ps).

Mean squared angular displacement

To calculate the mean squared angular displacement we used the spherical coordinate system (r,θ,ϕ) shown in Figure 12. In addition to the azimuthal angle, ϕ, and polar angle, θ, associated

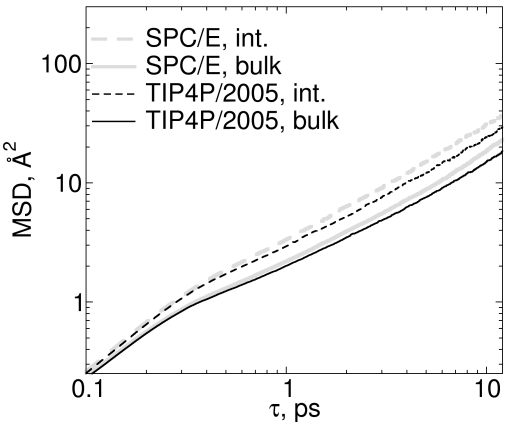

Figure 11: Mean squared displacement for SPC/E water molecules that at $t = 0$ are either at the interface or in the bulk.

with the spherical coordinate system we also use a third angle, ω, which is the angular distance between any two points at the surface of a sphere.

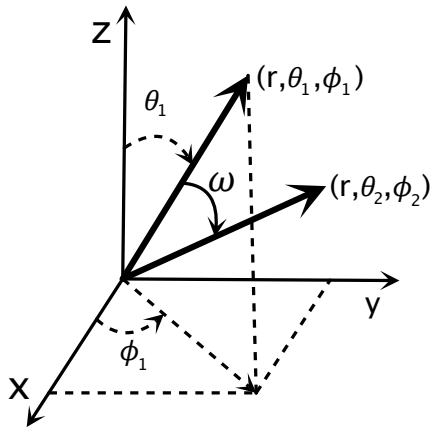

Figure 12: Coordinate system used to calculate the mean squared angular displacement. The OZ axis is perpendicular to the surface of the water slab. ω is the angle formed by two vectors of coordinates (r,θ_1,ϕ_1) and (r,θ_2,ϕ_2).

Here θ_t and ϕ_t denote the value of the corresponding angle at time t whereas $\theta(t)$, $\phi(t)$ or $\omega(t)$ denote angular differences measured with respect to θ_0, ϕ_0 or ω_0. The angle θ is a bounded quantity, so $\theta(t) = \theta_t - \theta_0$. In contrast, the angles ϕ and ω can vary between $-\infty$ and $+\infty$ and are calculated by unfolding the periodic trajectory described by each free OH group following

a procedure described previously.[15,16] This procedure requires that our free OH groups do not rotate by more than 180° between consecutive configurations. Here we ensure that this condition is met by taking configurations separated by only 4 fs. We describe the calculation of $\langle \omega(t)^2 \rangle$, the full MSAD; the calculation of the in-plane MSAD $\langle \phi(t^2) \rangle$ is analogous. Within a small time interval δt, a rotating OH group describes an angle $\delta\omega = |\omega_{t+\delta t} - \omega_t|$. We associate the angle $\delta\omega$ to a unit vector with direction given by $\hat{u}_t \times \hat{u}_{t+\delta t}$, where $\hat{u}$ is the unit vector that defines the orientation of an OH group. The angular displacement at time t is then given by a vector quantity, $\vec{\omega}(t) = \int_0^t \delta\vec{\omega}(t')dt'$. The mean square angular displacement is then calculated in the usual form by averaging over N OH groups:

$$\langle \omega(t)^2 \rangle = \frac{1}{N}\sum_i |\vec{\omega}_i(t) - \vec{\omega}_i(0)|^2 \tag{6}$$

Characteristic times associated with free-to-bonded and bonded-to-free transitions

As mentioned in the main text, transitions between stable free and bonded states are investigated through the $C(\tau)$ function. The resulting curves are fitted to biexponentials of the form $1 - e_1\exp(-x/e_2) - e_3\exp(-x/e_4)$. The parameters resulting from the fits are given in Table 1. It is noticeable that for each curve, long and short decay times differ by no more than a factor of three; the same trend is observed for the amplitudes of the exponentials. If this factor were at least 10, it would be reasonable to equate the characteristic times associated with free-to-bonded ($\tau_{f,b}$) or bonded-to-free ($\tau_{b,f}$) transitions with the times associated with the largest amplitude extracted from the fits. As this condition is not met, these characteristic times are calculated as the weighted average of the fitting parameters shown in Table 1: $\tau = (e_1e_2 + e_3e_4)/(e_1 + e_3)$.

Table 1: Fitting parameters for for free-to-bonded and bonded-to-free transitions (HB1 criteria for the bonded state, HB2 criteria for the free state).

	location	SPC/E	TIP4P/2005
e_1	interface	0.723	0.682
	bulk	0.797	0.748
e_2 (ps)	interface	0.654	0.739
	bulk	0.661	0.785
e_3	interface	0.281	0.321
	bulk	0.210	0.259
e_4 (ps)	interface	0.275	0.323
	bulk	0.292	0.342

References

(1) Jorgensen, W. L.; Chandrasekhar, J.; Madura, J. D.; Impey, R. W.; Klein, M. L. *J. Chem. Phys.* **1983**, *79*, 926–935.

(2) Abascal, J. L. F.; Vega, C. *J. Chem. Phys.* **2005**, *123*, 234505.

(3) Alejandre, J.; Chapela, G. A. *J. Chem. Phys.* **2010**, *132*, 014701.

(4) Impey, R. W.; Madden, P. A.; McDonald, I. R. *J. Phys. Chem.* **1983**, *87*, 5071–5083.

(5) Smith, D. E.; Dang, L. X. *J. Chem. Phys.* **1994**, *100*, 3757–3766.

(6) Taylor, R. S.; Dang, L. X.; Garrett, B. C. *J. Phys. Chem.* **1996**, *100*, 11720–11725.

(7) Kuo, I.-F. W.; Mundy, C. J.; Eggimann, B. L.; McGrath, M. J.; Siepmann, J. I.; Chen, B.; Vieceli, J.; Tobias, D. J. *J. Phys. Chem. B* **2006**, *110*, 3738–3746.

(8) Kühne, T. D.; Pascal, T. A.; Kaxiras, E.; Jung, Y. *J. Phys. Chem. Lett.* **2011**, *2*, 105–113.

(9) Stirnemann, G.; Rossky, P. J.; Hynes, J. T.; Laage, D. *Faraday Discuss.* **2010**, *146*, 263–281.

(10) Wilson, K. R.; Schaller, R. D.; Co, D. T.; Saykally, R. J.; Rude, B. S.; Catalano, T.; Bozek, J. D. *J. Chem. Phys.* **2002**, *117*, 7738–7744.

(11) Jedlovszky, P. *J. Phys.:Cond. Matter* **2004**, *16*, S5389–S5402.

(12) Cappa, C. D.; Smith, J. D.; Wilson, K. R.; Saykally, R. J. *J. Phys.:Cond. Matter* **2008**, *20*, 205105.

(13) Laage, D.; Hynes, J. T. *J. Phys. Chem. B* **2008**, *112*, 14230–14242.

(14) Vila Verde, A.; Campen, R. K. *J. Phys. Chem. B* **2011**, *115*, 7069–7084.

(15) Mazza, M. G.; Giovambattista, N.; Starr, F. W.; Stanley, H. E. *Phys. Rev. Lett.* **2006**, *96*, 057803.

(16) Mazza, M. G.; Giovambattista, N.; Stanley, H. E.; Starr, F. W. *Phys. Rev. E* **2007**, *76*, 031203.